Quantitative resonant tunneling spectroscopy: Current-voltage characteristics of precisely characterized resonant tunneling diodes

M. A. Reed, W. R. Frensley, W. M. Duncan, R. J. Matyi,[a] A. C. Seabaugh, and H.-L. Tsai

Central Research Laboratories, Texas Instruments Incorporated, Dallas, Texas 75265

A systematic comparison of precisely characterized resonant tunneling structures is presented. A self-consistent band bending calculation is used to model the experimentally observed resonant peak positions. It is found that the peak positions can be accurately modeled if the nominal characterization parameters are allowed to vary within the measurement accuracy of the characterization. As a result, it is found that the asymmetries in the current-voltage characteristics are solely explainable by tunnel barrier thickness fluctuations.

The origin of negative differential resistance in double barrier/single quantum well resonant tunneling structures is qualitatively well understood.[1] However, a full accounting of the current-voltage characteristics requires precise physical and electrical measurement of the device material properties. We present here a systematic comparison of measurements on precisely characterized resonant tunneling structures with models of the current-voltage dependence.

A set of four specimens has been grown by molecular beam epitaxy (MBE) to provide devices which vary over seven orders of magnitude in resonant peak current density for the AlGaAs/GaAs/AlGaAs system. This is achieved by growing nominally identical structures which differ solely in barrier thickness. Photoluminescence test structures were grown to provide for measurement of the AlGaAs band gap, transmission electron microscopy was used to independently verify the layer thicknesses, and capacitance-voltage profiling provided an independent determination of the doping density. The current-voltage characteristics of these structures have been measured. A systematic shift of the resonant peak and a variation of the resonant peak voltage asymmetry with current density is observed and compared with modeling results. It is found that a self-consistent band bending model can accurately predict the voltage peak positions, although the structural parameters used are not necessarily the "nominal" values, yet values within the error of the characterization measurement.

The samples used in this study were grown on Si-doped n^+-GaAs conductive substrates using a Riber 2300 MBE system. The structures consist of a 0.5 μm Si-doped GaAs buffer and bottom contact layer, a (nominally) 150 Å undoped GaAs spacer layer, an undoped AlGaAs tunnel barrier, an undoped GaAs quantum well, a second undoped AlGaAs tunnel barrier of nominally identical thickness, another 150 Å undoped GaAs spacer layer, a 0.5 μm Si-doped GaAs top contact, a 0.5 μm undoped AlGaAs layer, an undoped GaAs 50 Å quantum well, a 0.1 μm undoped AlGaAs layer, and a 100 Å GaAs cap layer. The entire structure was grown at constant temperature at 600 °C (to minimize Si diffusion) as measured by a short wavelength pyrometer.

The four specimens were grown sequentially to ensure a constant unintentional impurity background.

The active resonant tunneling structure is buried underneath a series of diagnostic photoluminescence structures. Conventional photoluminescence was performed at 4.2 and 300 K. The top quantum well photoluminescence exhibited typical full width at half maximum values of 10 meV. Photoluminescence of the thick AlGaAs layers was used for determination of the Al content. The band-gap relation of Casey and Panish[2] was assumed. The doping density of the n^+-GaAs layers was determined by standard capacitance-voltage profiling measurements, and the thicknesses of the tunnel barriers and quantum wells were determined by cross-sectional transmission electron microscopy (TEM). A summary of these structural parameters for the four samples studied is shown in Table I.

Prior to device fabrication, the top diagnostic layers were removed by a chemical etch so that contact could be made to the upper n^+-GaAs layer. Mesa devices ranging from 1.6×10^{-7} cm^{-2} to 4.1×10^{-5} cm^{-2} were fabricated by standard photolithography and chemical etching. Bonding pads contacted the upper top AuGeNi alloyed metal ohmic contact and a similar bottom contact through a Si_3N_4/polyimide passivation layer. Static current-voltage characteristics (four-point where necessary) were measured at 77 K.

Figure 1 shows a realistic conduction energy band profile of the 85 Å barrier thickness structure under (a) zero and (b) resonant bias. The model from which this figure was obtained finds the self-consistent solution of Poisson's equations for the electrostatic potential. The electrons in the con-

TABLE I. Summary of the structural parameters for the four resonant tunneling diode samples and the characterization techniques used.

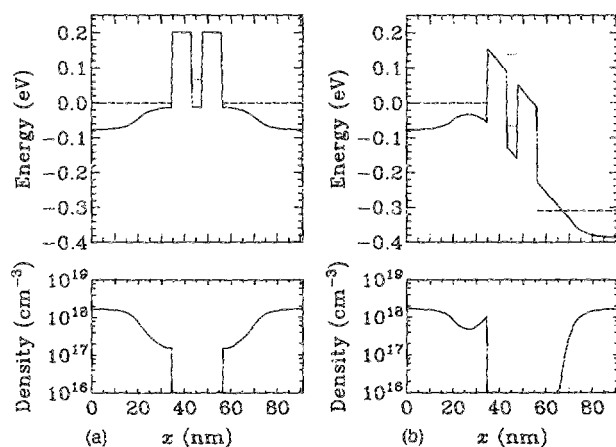| Barrier thickness (TEM)	RTD QW thickness (TEM)	Al content (PL, 300 K)	PL QW energy (PL, 4.2 K)	Contact doping density, cm^{-3} (CV)
118(± 5) Å	48(± 5) Å	27.7(± 0.6)	1.620 eV	1.7(± 0.2)10^{18}
85(± 5) Å	44(± 5) Å	26.4(± 0.6)	1.623 eV	1.7(± 0.2)10^{18}
65(± 5) Å	44(± 5) Å	27.7(± 0.6)	1.613 eV	1.4(± 0.4)10^{18}
32(± 5) Å	38(± 5) Å	25.0(± 0.6)	1.616 eV	2.6(± 0.1)10^{18}

FIG. 1. Self-consistent band diagram using Poisson's equations for the electrostatic potential. The electrons in the contacts are treated in a finite temperature Thomas–Fermi approximation. The simulation does not include current flow. The structure is an 85 Å $Al_xGa_{1-x}As$ ($x = 0.264$) barrier/44 Å GaAs QW/85 Å $Al_xGa_{1-x}As$ ($x = 0.264$) barrier structure at $T = 77$ K for (a) no applied bias and (b) resonant bias. The energies of the bound states are denoted by a dotted line and the Fermi level by dashed lines.

tacts are treated in a finite-temperature Thomas–Fermi approximation (i.e., these electrons are assumed to be in local equilibrium with the Fermi levels established by their respective electrodes). One result of this calculation, illustrated in Fig. 1(a), is that the band profile near the quantum well is significantly perturbed by the contact potential of the n^+-undoped junction. This shifts the resonant state upward (with respect to the n^+-GaAs Fermi level) from that expected from a naive flatband picture. This contact potential thus shifts the resonant peak position [Fig. 1(b)] considerably; the model predicts a resonant voltage at 310 meV, much higher than that predicted by a flatband picture.

Figure 2 shows the experimental current-voltage characteristics of a typical $(4 \mu m)^2$ mesa device of this structure at 77 K. Care must be exercised in the spectroscopy of the structures. Current-voltage characteristics of successively increasing mesa size (same epitaxial structure) progressively exhibit the well known plateau structure due to self-biasing.[3] This self-biasing perturbs and is observed to lower the apparent resonant peak position. For accurate spectroscopy, this effect must be avoided.
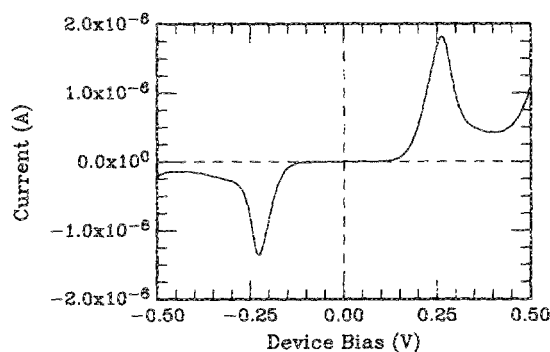
The experimental resonant peaks are not in very good agreement with the model calculation; the experimental peaks appear at 263 and 227 meV for positive and negative bias polarity, respectively, whereas the model predicts a value of 310 meV. (The convention here is that positive bias polarity implies electron injection from the top epitaxial contact.) What is also obvious is the asymmetry of the resonant peaks holds for both voltage and current. It is found that this asymmetry is not consistent for a large sampling of similar devices; the asymmetry ranges from zero to as much as 60 meV in voltage and a factor of 3.3 in current. However, the degree of asymmetry is correlated; a larger voltage asymmetry implies a larger current asymmetry.

To ascertain the degree of asymmetry and variation, characteristics of a large number of devices from the various epitaxial structures were measured. The resonant voltage peak positions as a function of resonant current density are shown in Fig. 3 (due to the above-mentioned complication of stabilizing oscillations, measurements from the 30 Å barrier were unreliable and are not presented here). The 118 Å barrier structure data exhibit a clear exponential behavior over two orders of magnitude, with the positive bias peaks occurring at lower voltages and current densities than the negative bias peaks. The 85 Å barrier structure data are not as clear, exhibiting considerable scatter. The origin of this scatter is not known. Additionally, the data exhibit the inverse of the 118 Å data; the positive bias peaks occur at higher voltages and current densities than the negative bias peaks. Finally, the 65 Å barrier structure deviates significantly from exponential behavior.

Examination of the 118 Å barrier structure data reveals the major cause of the asymmetry, both in current and voltage position. Consider a fluctuation in the thickness of one of the tunnel barriers of a nominal thickness barrier sample. This implies a change in the voltage position at which resonance occurs, and concurrently a change in the tunneling current. Figure 4 illustrates the 85 Å barrier structure with parameters varied *within* the error bars quoted in Table I; specifically, with the top barrier thickness equal to 80 Å, the bottom barrier thickness equal to 90 Å, and the quantum well equal to 48 Å. Figure 4(a) shows the modified structure under positive bias (the right-hand side of the figures corresponds to the top ohmic contact), and exhibits a resonant

FIG. 2. Current-voltage characteristics of the 85 Å sample for square mesa areas of 1.6×10^{-7} cm^2. Positive voltage corresponds to electron injection from the top contact. $T = 77$ K.
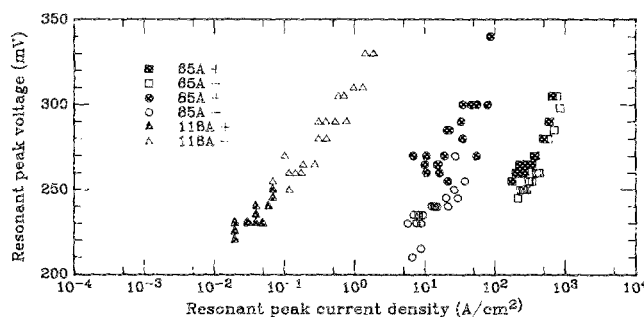

FIG. 3. Resonant peak voltage position vs resonant peak current density for a large sampling of three different barrier thickness structures. Both positive (+) and negative (−) voltage polarities are shown for the three structures of nominal barrier thickness 65, 85, and 118 Å. $T = 77$ K.
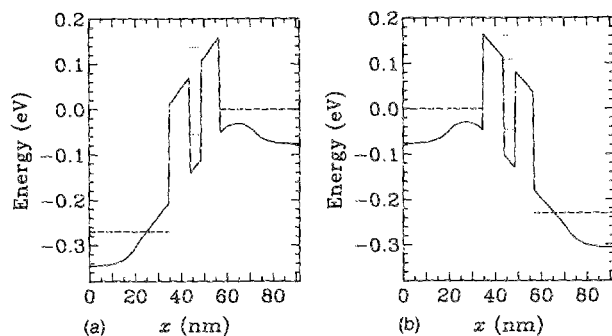
FIG. 4. Self-consistent band diagrams of a 90 Å bottm barrier/48 Å quantum well/80 Å top barrier structure at resonance. $T = 77$ K. (a) Positive bias and (b) negative bias polarities are the same as Fig. 2.

voltage at 270 meV. In the reverse bias direction [Fig. 4(b)], resonance occurs at 230 meV. These are in excellent agreement with experimentally observed values. Note that larger current densities correspond to electron injection first through the thinner (top) barrier.

Figure 3 shows that the inherently thinner top barriers of the 85 Å sample are a sample-dependent phenomenon; the 118 Å data reveal that the top barrier is thicker than the bottom barrier in the 118 Å sample. Likewise, the 65 Å sample appears to have approximately equal barrier thicknesses. These results imply that Si dopant redistribution, at least in these samples, is not a complication. Finally, the scatter in the 85 Å data with respect to the 118 and 65 Å data may imply that this sample has larger quantum well thickness fluctuations although this cannot be verified without further data on Al content and doping fluctuations.

The quantitative spectroscopy of these structures is rela-

tively straightforward if one stays in the regime where the structure impedance is dominated by the tunnel barriers. Outside of this regime (e.g., for the 65 Å data) the device may be affected by an internal series resistance. The resonant voltage position for the 65 Å data is found to be linear with current density, and gives a contact resistance of 8.8×10^{-5} Ω cm^2, equal for both positive and negative bias peak positions. This resistance can be fully accounted for by the AuGeNi ohmic metallization used here.

We have shown a self-consistent band bending model that can accurately predict experimentally observed resonant peak positions, and have compared it with precisely characterized resonant tunneling structures. It is found that, to accurately model the resonant voltage peak positions, the characterization values must be varied within the error bars of the measurement. Indeed, this technique can be used as an accurate diagnostic of the structure. Asymmetries in the electrical characteristics have been shown to be due to fluctuations in the tunnel barrier thicknesses.

[1]L. L. Chang, L. Esaki, and R. Tsu, Appl. Phys. Lett. 24, 593 (1974).
[2]H. C. Casey and M. B. Panish, *Heterostructure Lasers* (Academic, New York, 1978), pp. 187–194.
[3]J. F. Young, B. M. Wood, H. C. Liu, M. Buchanan, D. Landheer, A. J. SpringThorpe, and P. Mandeville, Appl. Phys. Lett. 52, 1398 (1988).